Lead-free halide perovskite photovoltaics: Challenges, open questions, and opportunities

Cite as: APL Mater. 8, 100901 (2020); doi: 10.1063/5.0022271
Submitted: 19 July 2020 • Accepted: 23 September 2020 •
Published Online: 5 October 2020

Vincenzo Pecunia,[1,a)] Luigi G. Occhipinti,[2,a)] Abhisek Chakraborty,[1] Yiting Pan,[3] and Yueheng Peng[1]

AFFILIATIONS

[1]Jiangsu Key Laboratory for Carbon-Based Functional Materials & Devices, Joint International Research Laboratory of Carbon-Based Functional Materials and Devices, Institute of Functional Nano & Soft Materials (FUNSOM), Soochow University, 199 Ren'ai Road, Suzhou, 215123 Jiangsu, China

[2]Department of Engineering, University of Cambridge, 9 JJ Thomson Avenue, Cambridge CB3 0FA, United Kingdom

[3]School of Architecture, Soochow University, 199 Ren'ai Road, Suzhou, 215123 Jiangsu, China

[a)]**Authors to whom correspondence should be addressed:** vp293@suda.edu.cn and lgo23@cam.ac.uk

ABSTRACT

In recent years, lead-free metal-halide perovskite photovoltaics has attracted ever-growing attention, in view of its potential to replicate the outstanding properties of lead-halide perovskite photovoltaics, but without the toxicity burden of the latter. Despite a research effort much smaller in scale than that pursued with lead-based perovskites, considerable progress has been achieved in lead-free perovskite photovoltaics, with the highest power conversion efficiencies now being in the region of 13%. In this Perspective, we first discuss the state of the art of lead-free perovskite photovoltaics and additionally highlight promising directions and strategies that could lead to further progress in material exploration and understanding as well as in photovoltaic efficiency. Furthermore, we point out the widespread lack of experimental data on the fundamental optoelectronic properties of lead-free halide perovskite absorbers (e.g., charge carrier mobility, defect parameters, Urbach energy, and the impact of dimensionality). All of this currently hampers a rational approach to further improving their performance and points to the need for a concerted effort that could bridge this knowledge gap. Additionally, this Perspective brings to the fore the manifold photovoltaic opportunities—thus far largely unexplored with lead-free perovskite absorbers—beyond single-junction outdoor photovoltaics, which may potentially enable the realization of their full potential. The exploration of these opportunities (tandem photovoltaics, indoor photovoltaics, and building-integrated and transparent photovoltaics) could energize the investigation of existing and new classes of lead-free perovskite absorbers beyond current paradigms and toward high photovoltaic performance.

I. INTRODUCTION

Over the past decade, lead-halide perovskites have reached prominence in photovoltaics and beyond,[1–6] delivering a tremendous rise in single-junction power conversion efficiency (PCE) (now greater than 25%)[7] through remarkably simple manufacturing processes. Apart from instability issues currently being tackled,[8] their reliance on toxic lead is a fundamental limiting factor preventing lead-halide perovskite photovoltaics from reaching commercial maturity as an alternative to silicon-based photovoltaics. This has spurred researchers to look for alternative metal-halide perovskite absorbers with closely related properties yet lead-free.[9] Prominent classes of such absorbers comprise tin-based and germanium-based perovskites and derivatives, antimony-based and bismuth-based perovskite derivatives, and double perovskites. Considerable progress has been recently achieved in this area—with their highest single-junction PCE now at 13.2%—despite a research effort incomparably smaller in scale and spanning a much shorter time than lead-based perovskite photovoltaics research.

This Perspective provides a timely fresh look at the status and prospects of the rapidly evolving area of lead-free perovskite absorbers for photovoltaics. It first surveys the main classes of lead-free metal-halide perovskite absorbers—tin-based, germanium-based, bismuth-based, and antimony-based and halide double perovskites (HDPs)—highlighting the most promising solutions explored to date. This is followed by a discussion of the most

important challenges in lead-free perovskite photovoltaics, with a particular focus on photovoltaic efficiency and stability characterization. General strategies that may enable these challenges to be overcome are also jointly discussed. Subsequently, this Perspective highlights key outstanding questions in the area of lead-free perovskite absorbers for photovoltaics, identifying as a priority area the detailed investigation of their charge transport and defect properties, as well as the role of dimensionality. Finally, this Perspective looks at the opportunities beyond single-junction solar harvesting that could realize the full photovoltaic potential of lead-free perovskites in the near future.

II. STATUS OF LEAD-FREE PEROVSKITE PHOTOVOLTAICS

In this section, we provide an overview of the status of photovoltaics research based on lead-free perovskite absorbers, highlighting the most recent developments. While a very large number of lead-free perovskite absorbers have been pursued to date, our discussion focuses on the material families that have attracted the most interest because of their photovoltaic potential, i.e., tin-based and germanium-based perovskites and derivatives, antimony-based and bismuth-based perovskite derivatives, and double perovskites (see Fig. 1 for their structures and constituents).

A. Tin-based perovskites and derivatives

A mainstream strategy for lead-free perovskite photovoltaics involves the replacement of lead with same-group tin.[10] The resulting tin-based perovskites and derivatives have been central in lead-free perovskite photovoltaics, thus far delivering the highest PCE (13.24%).[11]

Since Sn^{2+} has a similar ionic radius as Pb^{2+}, tin allows the formation of $ASnX_3$ perovskites (with A being a monovalent cation and X being a halide anion), which possess a three-dimensional (3D) structure analogous to that of the mainstream lead-based perovskites [Fig. 1(a)]. $MASnI_3$ [MA: methylammonium, see Fig. 1(h)], $FASnI_3$ [FA: formamidinium, see Fig. 1(h)], and $CsSnI_3$ have been at the forefront of tin-based perovskite research. In addition to their structural and optoelectronic similarity with their lead-based counterparts, the attractiveness of these absorbers relates to their direct gaps in the region of 1.3 eV–1.4 eV [see Fig. 2(a) for their absorption spectra],[12] which are ideal for single-junction photovoltaics. The resulting solar cells have delivered excellent short-circuit current (in many instances >20 mA cm^{-2}) but have generally suffered from low open-circuit voltage V_{oc} (often in the range of 0.3 V–0.4 V), leading to PCE values typically <7%.[12] This has been traced to several issues, most importantly (a) the inherent tendency of Sn^{2+} to oxidize into Sn^{4+}, leading to severe device instability and a large carrier background due to concurrent *p*-type doping,[13,14] and (b) a high defect density due to morphological imperfections.[15] An approach that has been widely pursued to mitigate the instability issue involves the use of reducing agents as additives.[16–19] This has led to PCE values up to ~10% [Fig. 2(e)] and improved stability, the latter being, nonetheless, unsuitable for real-world applications[18,19] (e.g., a PCE reduction of 30% after hundreds of minutes in low relative humidity[19]). Most recently, PCE values up to 13.24% [Fig. 2(e)]—the highest to date for all lead-free perovskite absorbers—have been achieved through defect passivation and lattice-strain reduction.[11,20,21]

In order to overcome the issues faced by $ASnX_3$ photovoltaics, a number of alternative tin-based approaches have been pursued based on the manipulation of the perovskite structure. One such approach involves tin-based vacancy-ordered (VO) double perovskites, which manifest superior stability but have achieved rather low PCE to date (see Sec. II D). Another notable route involves "hollow" perovskites, in which medium-sized cations are used to produce structural voids within a 3D perovskite structure [Fig. 1(b)].[22] This has resulted in promising PCE values [~7%, see Fig. 2(e)] and improved stability compared to additive-free $ASnX_3$.[23] Higher

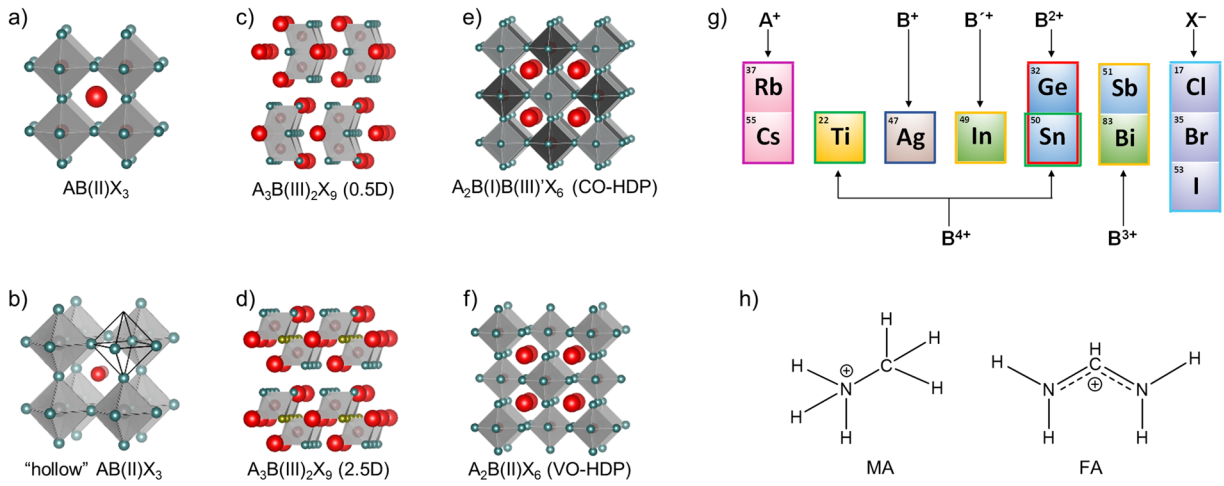

FIG. 1. Lead-free halide perovskites: (a)–(f) common structures; common (g) inorganic and (h) organic constituents.

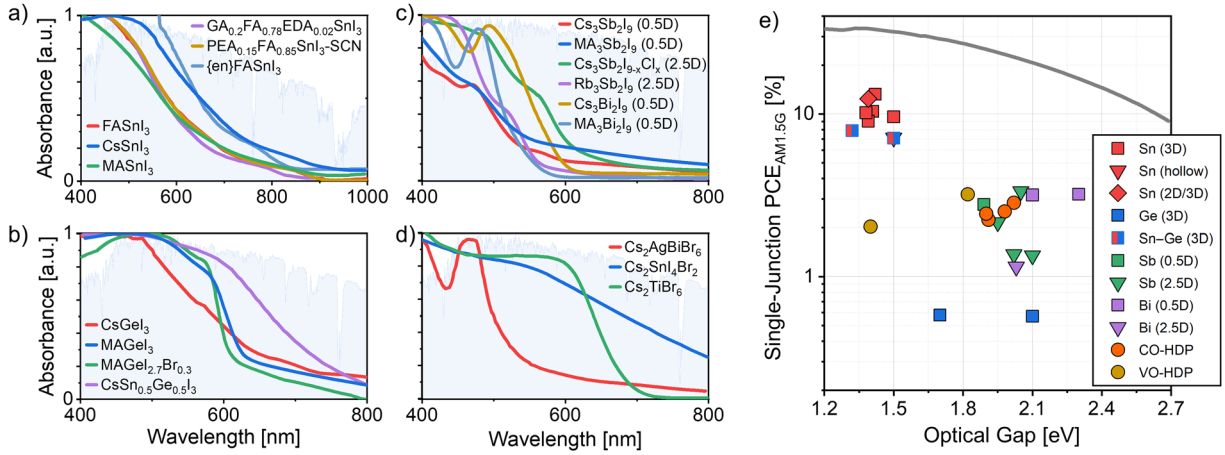

FIG. 2. Normalized absorbance of representative materials: (a) tin-based;[18,20,23,25,33,34] (b) germanium-based;[29–31] (c) antimony-based and bismuth-based;[35–38] (d) double perovskites.[39–41] The AM 1.5G spectrum is overlaid for the sake of comparison. (e) Single-junction PCE under AM 1.5G illumination vs optical gap of representative absorbers (solid symbols);[11,18,20,21,23,25,29–32,35,37,39–50] single-junction theoretical solar cell efficiency under AM 1.5G illumination in the Shockley–Queisser limit (line).

PCE values have been achieved through dimensional manipulation, with a particularly promising route involving "2D/3D" perovskites, in which 3D domains are mixed with layered (i.e., quasi-two-dimensional) domains.[24–26] In fact, the bulky cations of the layered phase have been identified as conducive to enhanced stability.[27] PCE values in the region of 9% and up to 12.4% have been achieved with the latter approach[24–26] [Fig. 2(e)], along with a shelf-life of 3800 h for encapsulated devices.[25]

B. Germanium-based perovskites and derivatives

The interest in germanium-based perovskites arises from the electronic similarity of Ge^{2+} with Pb^{2+}, which enables the formation of structurally 3D $AGeX_3$ perovskites (with A being a monovalent cation and X being a halide anion).[1] In regard to single-junction photovoltaics, the most promising candidate has been identified in $CsGeI_3$, due to its direct gap of 1.63 eV [Fig. 2(b)].[28] The use of lighter halogens or alternative A-site cations leads to wider bandgaps [e.g., 2.0 eV for $MAGeI_3$, see Fig. 2(b)].[28,29]

Despite their high theoretical single-junction efficiency in the Shockley–Queisser limit (e.g., ≈30% for $CsGeI_3$), very few reports on germanium-based-perovskite photovoltaics have appeared to date. This can be traced to the pronounced instability arising from the tendency of Ge^{2+} to oxidize into Ge^{4+}.[28] The highest reported PCE is ~0.6% [Fig. 2(e)] and has been achieved through compositional engineering and morphological improvements of the perovskite layers.[29,30]

An alternative direction in Ge-based-perovskite photovoltaics involves absorbers in which germanium is alloyed with tin, leading to $ASn_{1-x}Ge_xX_3$. A particularly promising result was obtained with $CsSn_{0.5}Ge_{0.5}I_3$, which delivered a PCE of 7.11% [Fig. 2(e)] along with improved stability with respect to the $CsSnI_3$ case.[31] This was attributed to the enhanced stability resulting from alloying and to the passivating effect of the native germanium oxide formed at the perovskite surface and interfaces. Moreover, the trap-healing effect of germanium in $FA_{0.75}MA_{0.25}Sn_{1-x}Ge_xI_3$ was recently shown to deliver a PCE of 7.9% [Fig. 2(e)].[32]

C. Antimony-based and bismuth-based perovskite derivatives

Antimony and bismuth have emerged as attractive for the development of lead-free perovskite absorbers due to their low toxicity and the electronic similarity of their 3+ cations with Pb^{2+}.[51] $A_3B_2X_9$ absorbers (B^{3+} = Sb^{3+} or Bi^{3+}) may come in two different phases: a dimer phase (0.5-dimensional, i.e., 0.5D, following Xiao *et al.*)[52] featuring isolated face-sharing metal-halide bi-octahedra [Fig. 1(c)] and a layered phase (2.5-dimensional, i.e., 2.5D, following Xiao *et al.*)[52] featuring planes of corner-sharing metal-halide octahedra [Fig. 1(d)].[53] Research efforts have primarily focused on 0.5D ternary iodide absorbers ($A_3B_2I_9$, with A = Cs^+, MA^+), which have bandgaps in the region of 2.1 eV–2.4 eV [Fig. 2(c)].[54–56] While this points to considerable potential for tandem photovoltaics (see Sec. IV), research on 0.5D Sb-based and Bi-based absorbers to date has narrowly focused on single-junction photovoltaics. While the majority of the early studies on 0.5D absorbers delivered rather modest PCE (<1%),[54,56,57] recent developments—building on the use of additives,[35,58] optimized transport layers,[35] or dedicated deposition protocols[45,46]—have led to significant performance improvement, with the PCE reaching 2.8% for 0.5D $MA_3Sb_2I_9$ and 3.2% for 0.5D $A_3Bi_2I_9$ (A = Cs^+, MA^+) [Fig. 2(e)],[35,45,46] in some instances also with excellent device stability in air (e.g., non-encapsulated devices retaining 97% of their initial PCE over a period of 60 days).[45]

The higher dimensionality of 2.5D antimony-based and bismuth-based $A_3B_2X_9$ absorbers makes them more attractive for photovoltaics, also in view of their narrower bandgaps [Fig. 2(c)] and smaller exciton binding energy and effective masses.[55,59] While mainstream $MA_3B_2I_9$ and $Cs_3B_2I_9$ (B^{3+} = Sb^{3+}, Bi^{3+}) come in the 0.5D phase when deposited through conventional methods, 2.5D

$A_3M_2X_9$ absorbers have been demonstrated through dedicated processing protocols,[59–61] or halide mixing,[37,43,62] or the use of smaller A-site cations such as Rb^+.[38,63] A PCE of 1.4% has been achieved with 2.5D $Rb_3Sb_2I_9$ [Fig. 2(e)], with both a mesoporous and a planar device structure.[38,47] Moreover, PCEs of 2.2% and 3.34% have been recently obtained with 2.5D $Cs_3Sb_2Cl_xI_{9-x}$ and $MA_3Sb_2Cl_xI_{9-x}$, respectively [Fig. 2(e)].[37,42]

D. Halide double perovskites (HDPs)

Cation-ordered halide double perovskites (CO-HDPs) have attracted significant attention in view of their nominally appealing three-dimensional structure. They have a general formula $A_2BB'X_6$, where B and B′ are a monovalent cation and a trivalent cation, respectively, alternating at the octahedra centers of a perovskite lattice [while A is a monovalent cation and X is a halide anion, see Fig. 1(e)].[64] Additionally, HDPs comprise vacancy-ordered (VO) embodiments, with a general formula A_2BX_6 and featuring the alternation of a tetravalent cation B^{4+} and a B-vacancy at the octahedra centers of a perovskite lattice [Fig. 1(f)].[65] Therefore, in contrast to cation-ordered HDPs, vacancy-ordered HDPs are structurally quasi-zero-dimensional (quasi-0D), in consideration of the fact that neighboring $[BX_6]^{2-}$ octahedra are isolated from one another.[66]

Cation-ordered HDPs constitute a very broad material class, with more than 350 compounds synthesized to date and many more predicted.[67] Photovoltaics research has primarily focused on silver–bismuth HDPs such as Cs_2AgBiX_6 (X = Cl or Br). Due to their large and indirect gaps (2 eV–2.3 eV) as well as the presence of obvious excitonic features [see Fig. 2(c)],[65,68] these absorbers do not represent the ideal choice for single-junction photovoltaics. For instance, the single-junction spectroscopic limited maximum efficiency (which quantifies the maximum achievable efficiency taking into account the magnitude of the absorption coefficient and the nature of the bandgap)[69] for $Cs_2AgBiBr_6$ is ~8%.[70] In fact, despite their 3D structure, these cation-ordered HDPs are electronically 0D, as the orbitals contributing to their band edges are spatially isolated.[52] Their low-toxicity profile and 3D structure have nonetheless prompted their investigation for photovoltaics, also encouraged by their long carrier lifetimes (≈600 ns)[48,71] and outstanding stability in air (e.g., non-encapsulated devices showing no obvious PCE degradation after 30 days in air).[72] The highest PCE values in single-junction devices to date are in the region of 2.2%–2.8% [Fig. 2(e)],[40,48–50] with the highest performance being achieved in combination with an organic interlayer that slightly increases the overall photon absorption beyond the onset of the perovskite absorber.[49]

Owing to the limitations of the Cs_2AgBiX_6 (X = Cl, Br) system, research efforts in HDP photovoltaics have also been directed at the synthesis and assessment of alternative cation-ordered HDPs with narrower gaps. While using iodine as the halogen in Cs_2AgBiX_6 could potentially deliver in this direction, Cs_2AgBiI_6 has been generally dismissed due to thermodynamic instability considerations.[73] However, recent progress in the synthesis of colloidal Cs_2AgBiI_6 nanocrystals with a bandgap of 1.75 eV indicates that Cs_2AgBiI_6 offers a promising opportunity.[74] An alternative approach that has attracted attention involves the substitution of bismuth with antimony. A representative compound of this class is $Cs_2AgSbBr_6$, which delivers an indirect gap of ~1.64 eV, yet the PCE reported to date is rather poor (0.01%).[75] Another system that has been proposed is Cs_2AgInX_6, which has a direct gap, yet associated with an undesirable parity-forbidden transition.[76]

Vacancy-ordered HDP research has thus far focused on Cs_2SnX_6 and Cs_2TiBr_6. In contrast to the case of $ASnX_3$ perovskites, tin is present in its stable 4+ oxidation state in Cs_2SnX_6 compounds, thus making them more robust against degradation. With a direct gap of 1.3 eV–1.6 eV [Fig. 2(d)],[12] Cs_2SnX_6 absorbers inherently overcome the issues thus far affecting cation-ordered HDPs, and their Shockley–Queisser efficiency limit for single-junction photovoltaics is greater than 25% [Fig. 2(e)].[77,78] The highest PCE achieved with Cs_2SnX_6 to date amounts to 2.0% [Fig. 2(e)] and has been demonstrated along with promising stability in air (a reduction of only ~5% of the original PCE in encapsulated devices during a period of 50 days).[39] Nonetheless, the quasi-0D structural and electronic nature of Cs_2SnX_6 absorbers (with associated large effective masses)[52] may hamper further progress in their photovoltaic performance. Another attractive vacancy-ordered HDP is titanium-based Cs_2TiBr_6, which has been shown to deliver a promising PCE of 3.3% [Fig. 2(e)] in single-junction devices along with good environmental stability (non-encapsulated devices retain 94% of their initial PCE after 14 days at 70 °C in air and under ambient illumination), building on a quasi-direct gap of 1.8 eV [Fig. 2(d)] and a carrier diffusion length >100 nm.[41] While these results have been recently brought into question,[79] research on the vacancy-ordered A_2TiX_6 system is still at its infancy, and many such compounds have never been synthesized to date—which points to the need for further investigation of this area.

III. CHALLENGES AND OPEN QUESTIONS

Despite the considerable advances in recent years (Sec. II), further progress in both photovoltaic efficiency and stability is needed for lead-free perovskite photovoltaics to approach commercial exploitation. In the following (Secs. III A and III B), we provide our perspective on both of these aspects, discussing the associated challenges and potential solutions, wherever relevant. Subsequently, we highlight some key open questions concerning charge transport (Sec. III C), defect tolerance (Sec. III D), and dimensionality (Sec. III E), whose investigation is critical in order to catalyze further progress in lead-free perovskite photovoltaics.

A. Photovoltaic efficiency

Tin-based perovskites motivate further efforts in their exploration for use in single-junction solar cells. While they have achieved the highest photovoltaic performance to date (13.24%) of all lead-free perovskites, their bandgap values point to a single-junction Shockley–Queisser efficiency limit of ~32% [Fig. 2(e)], thereby suggesting considerable scope for improvement. Importantly, the short-circuit current of the best performing tin-based perovskite solar cells to date is consistently close to the Shockley–Queisser limit (Fig. 3), indicating efficient photocarrier generation and collection at the contacts. The gap between the reported performance of $ASnX_3$ cells and their Shockley–Queisser limit can be traced to a V_{oc} deficit of ~0.4 V, as shown in Fig. 3.[11] This V_{oc} deficit can be attributed to a high defect density, which leads to non-radiative recombination—as

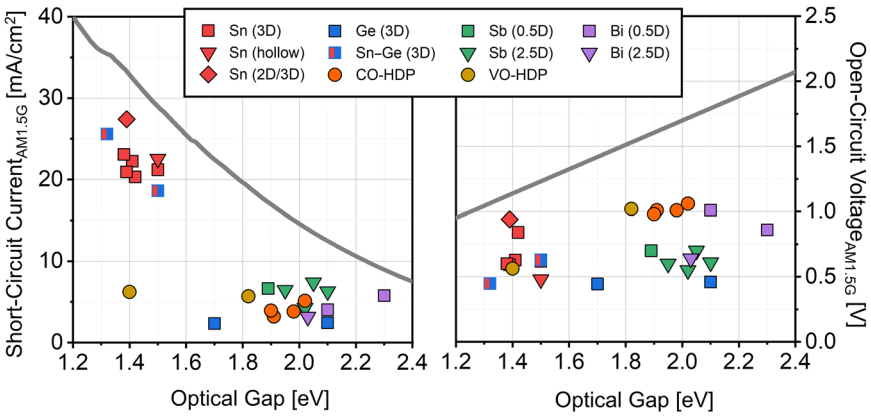

FIG. 3. Reported short-circuit current (left) and open-circuit voltage (right) of representative lead-free perovskite solar cells under AM 1.5G illumination.[11,18,20,21,23,25,29–32,35,37,39–50] The short-circuit current and open-circuit voltage in the Shockley–Queisser limit (for single-junction devices under AM 1.5G illumination) are also shown for the sake of comparison.

also confirmed by the fact that the best performing devices have an ideality factor $1 < n < 2$.[11] All of this indicates that the outstanding challenge in $ASnX_3$ photovoltaics research concerns the development of refined defect passivation protocols. Based on recent developments, it can be envisaged that this should not be pursued through standalone strategies, but instead through a holistic approach. Defect passivation protocols should combine the compositional and morphological optimization of the photoactive layer (through A-site cation mixing and additive incorporation), the enhancement of its stability against oxidation, and the use of a dedicated device stack that minimizes interfacial recombination. In particular, 3D systems with mixed cations and mixed 2D/3D systems are highly promising in order to achieve low defect density and good stability, provided that additives are also used to aid film formation and enhance crystallinity.

In addition to non-radiative losses, future efforts in tin-based perovskite research should also be directed at ascertaining and tackling the V_{oc} deficit associated with their energetic disorder. For the sake of illustration, Jiang *et al.* recently reported that their optimized tin-based perovskite films (which deliver one of the highest PCEs, i.e., 12.4%, and a record-high V_{oc} of 0.94 V) have an Urbach energy of 65 meV,[25] which is expected to result in a V_{oc} deficit of several hundreds of meV.[2] It is worth noting that significantly lower Urbach energy values (16 meV–32 meV) were observed from $CsSnI_{3-x}Br_x$, albeit in association with a much lower V_{oc}.[80] Considering that energetic disorder has been seldom reported in the tin-based perovskite literature, it is apparent that an important priority is to explore the impact of processing and composition on the energetic disorder and the associated V_{oc} deficit of tin-based perovskites.

Germanium-based $AGeX_3$ perovskites have thus far delivered the lowest PCE of all lead-free perovskite systems discussed herein [Fig. 2(e)]. Their particularly low performance is jointly due to significant losses in both V_{oc} ($V_{oc} \approx 0.5$ V) and J_{sc} ($J_{sc} \approx 2$ mA/cm^2) (Fig. 3). The particularly low efficiency of germanium-based $AGeX_3$ perovskite solar cells can be traced to the presence of deep levels,[29,81] in addition to their rapid degradation due to oxidative instability. All of this indicates a considerable analogy with additive-free $ASnX_3$ perovskites, suggesting that future efforts in $AGeX_3$ photovoltaics may require the development of material stabilization protocols as well as defect-healing strategies based on additives and compositional engineering.

Tin–germanium perovskites have achieved much higher efficiencies than the germanium-only system (i.e., $AGeX_3$). Their PCE values (~7%) are significantly lower than the Shockley–Queisser limit, however [Fig. 2(e)]. Their J_{sc} is in a similar range as the tin-based counterparts (Fig. 3), thereby leaving some scope for improvement. However, the major challenge with tin–germanium perovskites to date is their V_{oc} deficit, which is greater than 0.5 V (Fig. 3). Considering that the recently reported increase in the efficiency of tin–germanium perovskite solar cells has been traced to a stability enhancement against oxidation as well as to trap passivation,[31,32] it can be foreseen that tin–germanium perovskite solar cells could potentially deliver higher efficiency through the adoption of a holistic approach to trap passivation and stabilization (along similar lines as pursued with $ASnX_3$). In addition to non-radiative recombination losses, however, the reported large Urbach energy (in the region of 50 meV for polycrystalline thin films)[82] points to the urgency of also reducing the energetic disorder as a means of boosting V_{oc} and the overall PCE.

Despite the recent progress in antimony-based and bismuth-based $A_3B_2X_9$ perovskite derivatives, their photovoltaic performance is still appreciably lower than their Shockley–Queisser limit—with no significant difference between antimony-based and bismuth-based absorbers [Fig. 2(e)]. Their J_{sc} is significantly lower than the Shockley–Queisser limit (Fig. 3), indicating significant losses in charge generation and/or collection, notwithstanding the widespread use of a mesoporous device structure. However, in one particular instance in which a 2.5D system ($Rb_3Sb_2I_9$) was employed, a J_{sc} up to ≈50% of the Shockley–Queisser limit was reached (Fig. 3), remarkably with a planar device structure.[38] In terms of V_{oc}, the gap between the reported values and the corresponding Shockley–Queisser limit is significantly more severe (often >1 V), with 0.5D bismuth-based systems performing better than 0.5D and 2.5D antimony-based systems (Fig. 3). Additionally, while 2.5D systems have been generally regarded as superior (e.g., they can provide improved charge transport within their sheets of octahedra and are expected to be more defect-tolerant),[55,59,83] interestingly, such systems have only been investigated in very few instances. Notably, all 2.5D antimony-based and bismuth-based embodiments

have been explored with their sheets of octahedra either predominantly parallel to the substrate or randomly aligned,[37,38,42,43,47,55,59,63] likely resulting in enhanced recombination losses. Therefore, it can be envisaged that their efficiency could be significantly improved by further exploring 2.5D $A_3B_2X_9$ systems—in particular by developing deposition strategies for the realization of films with the sheets of octahedra aligned in the out-of-plane direction.[37,38] Additionally, while the energetic disorder has been scarcely characterized in bismuth-based and antimony-based absorbers, Urbach energy values in the region of 60 meV or larger have been reported for some of these materials.[56,63] This indicates the future efforts in reducing the V_{oc} deficit should also aim at improving composition, deposition conditions, and device structures toward the minimization of the energetic disorder.

The efficiency of cation-ordered Cs_2AgBiX_6 HDPs thus far has been well below the Shockley–Queisser limit for single-junction cells [Fig. 2(e)]. This is primarily determined by a considerably low J_{sc}, which is often less than 1/3 of the Shockley–Queisser limit, while the V_{oc} deficit has been comparatively moderate (in some instances of ≈0.6 V) (Fig. 3). The J_{sc} deficit can be traced to the indirect gap of the cation-ordered double perovskites explored to date, which leads either to a suboptimal light collection for particularly thin films or to an inefficient charge collection for thicker films intended to boost light absorption. Additionally, their absorption spectra manifest obvious excitonic effects near the absorption edge [Fig. 2(d)], which may further reduce the photogeneration efficiency. Therefore, the search is still open for alternative cation-ordered HDPs inherently suitable for single-junction photovoltaics—especially with a direct gap and with a higher electronic dimensionality than electronically 0D Cs_2AgBiX_6—confirming that this area is at its infancy. Considering the wealth of additional absorbers that have been predicted (some of which are expected to have desirable optoelectronic properties)[76] but have not been explored to date, further progress in cation-ordered HDPs requires first and foremost the synthesis and characterization of such materials. Furthermore, despite their smaller direct gaps, vacancy-ordered HDPs have also delivered PCE and J_{sc} values much lower than the Shockley–Queisser limit [Figs. 2(e) and 3]. While research on vacancy-ordered HDPs is still in its nascent stage and further optimization of the synthesis and deposition conditions may be needed to boost their photovoltaic performance, current indications of their defect-intolerance and poor charge transport may ultimately limit the scope of these efforts.[66]

Regardless of the specific lead-free perovskite considered, photovoltaic performance is influenced considerably by the morphology of the photoactive layer. This aspect is of primary importance because the photoactive layers employed in lead-free perovskite photovoltaics are generally polycrystalline and typically deposited through solution-based methods. Control of the processing conditions (e.g., solvent selection, solution concentration, and annealing temperatures) and the specific methodology adopted (e.g., one-step spin-coating, antisolvent processing, solvent-vapor annealing) are, therefore, key to obtaining, first of all, compact and uniform films, given that pinholes are detrimental to photovoltaic efficiency due to their shunting effect.[84] Additionally, grain boundaries are to be minimized, as they provide a barrier to charge transport and may also contain a high density of defect states acting as recombination centers. The deposition of high-quality films (i.e., compact and with grain size in the region of 1 μm) of tin-based perovskites requires considerable efforts (e.g., solvent engineering and the identification and optimization of suitable additives),[18,20] given the fast crystallization rate of such perovskites during solution processing.[12] This endeavor has allowed tin-based perovskites to reach a film quality approaching that of state-of-the-art lead-based perovskites,[85,86] thereby playing an important role in enabling them to deliver the highest efficiencies among lead-free perovskites.[18,44] By contrast, the film morphology of other classes of lead-free perovskites is yet to approach similar levels. For instance, in the case of double perovskite $Cs_2AgBiBr_6$, progress in photovoltaic efficiency has been achieved through films with grain size in the region of 400 nm, which were obtained through the optimization of antisolvent processing and high-temperature annealing.[40] In the case of Bi-based and Sb-based $A_3B_2X_9$ absorbers, research efforts have primarily relied on films with suboptimal morphology, with grain size often much less than 100 nm and/or imperfect coverage.[35,37,45,46] While the challenge of depositing films of Bi-based and Sb-based $A_3B_2X_9$ absorbers without a large number of pinholes has been addressed through several methods (e.g., dissolution–recrystallization,[46] solvent-vapor annealing,[37] vapor assisted solution process[45]), the grain size of the resultant films is well below 1 μm. As illustrated by the work of Li *et al.* for the case of $Rb_3Sb_2I_9$,[38] boosting the grain size of such perovskite derivatives has a considerable impact on the photovoltaic performance and requires dedicated processing protocols (e.g., reduced-supersaturation annealing and high-temperature vapor annealing) that strike a balance between crystallization and nucleation rates. This generally represents an outstanding challenge in cation-ordered double perovskites and Bi-based and Sb-based $A_3B_2X_9$ photovoltaics. Therefore, it can be envisaged that a considerable enhancement in their photovoltaic efficiency could be realized through the development of processing protocols delivering films with grain size in the micrometer range.

As a final point on the challenges thus far encountered with regard to the photovoltaic efficiency of lead-free perovskite absorbers, interfacial recombination and inefficient extraction at the transport layers and contacts may also be currently limiting their photovoltaic performance—in addition to the bulk recombination properties discussed earlier. This relates to the choice of transport layers, which are typically drawn from lead-based perovskite research, hence may be suboptimal for lead-free perovskite absorbers. Therefore, further progress in the photovoltaic efficiency of lead-free perovskites will also require the investigation of interfacial recombination effects and the exploration and optimization of dedicated charge transport layers.

B. Stability

The search for inherently stable absorbers—beyond the limitations of mainstream lead-halide perovskites—has been an important driving force in the exploration of lead-free halide perovskites. While several solutions have been developed over time to improve the stability of inherently unstable Sn^{2+}-based absorbers (see Sec. II A), many double perovskites as well as bismuth-based and antimony-based $A_3B_2X_9$ absorbers have demonstrated inherent stability, based on indications from both thin-film properties and device performance (see Secs. II C and II D). In fact,

an important remaining challenge in the development of stable lead-free perovskite solar cells suitable for commercialization (aside from the obvious efficiency requirements) arises from the diversity of approaches that have been used to date to characterize their photovoltaic stability. This has been particularly limiting because it has prevented (a) the benchmarking of the photovoltaic stability of the manifold lead-free absorbers explored to date; (b) the identification of the best candidates for highly stable lead-free perovskite photovoltaics; and (c) the assessment of the gap that still needs to be bridged for lead-free perovskite photovoltaics to approach commercialization. In light of the standardized protocols for the stability characterization of halide perovskites that have been proposed recently,[87] it is therefore highly desirable that future studies on lead-free perovskite photovoltaics may assess stability through these protocols. Indeed, this would pave the way for a systematic understanding of stability issues in lead-free perovskite absorbers, ultimately enabling the optimization of systems with a promising stability profile toward commercialization-ready levels.

C. Defect parameter characterization and experimental screening for defect tolerance

A guiding light in the search for lead-free perovskite absorbers with promising optoelectronic potential has been the development of absorbers that may have a defect-tolerant character, i.e., insensitivity to the defects inevitably present in low-temperature-deposited semiconductor thin films. In electronic terms, defect-tolerant semiconductors may present defect states that either are shallow and with small capture cross sections or fall within the energy bands.[88] Extrapolating from lead-halide perovskite studies, the search for defect-tolerant lead-free perovskite absorbers has targeted materials based on large, highly polarizable metal cations with ns^2 outer orbitals.[88–90] In this regard, computational studies have offered highly valuable indications on the compositions that are potentially most promising from the point of view of defect tolerance.[91,92] However, conclusive evidence on the defect tolerance of the manifold classes of lead-free perovskite absorbers should be sought experimentally—as a means of validating the indications drawn from computational studies as well as a tool to rationally develop compositions and deposition strategies for higher photovoltaic performance. In fact, the experimental assessment of defects in lead-free perovskites has been primarily phenomenological to date, relying on techniques that provide only a measure of the total volumetric defect density (e.g., basic space-charge-limited-current characterization),[40,60,93] or on indicators that largely relate to defect tolerance but do not constitute a univocal measure of the same (e.g., photoluminescence lifetime).[19,20,94] By contrast, a thorough experimental evaluation of defect tolerance in lead-free perovskite absorbers—in terms of defect densities, characteristic energies, and capture cross sections—has not been pursued to date. Importantly, the experimental assessment of the defect properties of lead-free perovskite absorbers would aid the identification of those that have high photovoltaic potential and concurrently offer rational criteria for the development of processing protocols for defect state passivation. Therefore, the investigation of experimental approaches for the characterization of the defect parameters of lead-free perovskites is a key priority in lead-free perovskite photovoltaics research.

D. Charge transport characterization

Charge transport plays an essential role in photoconversion, allowing photocarriers to be collected prior to undergoing recombination. Therefore, charge transport data on lead-free perovskite absorbers are of primary importance in order to rationally approach the optimization of their photovoltaic performance. However, experimental charge transport data reported to date from lead-free perovskites are sparse and incomplete, ultimately preventing the identification of relevant trends and hampering the development of solutions for high-performance photovoltaics.

Most experimental charge transport data on lead-free perovskites have been obtained through space-charge-limited current (SCLC) characterization. Importantly, SCLC data are typically presented in the single-sweep mode (e.g., forward scan only), preventing the appraisal of any possible hysteretic effects and other non-idealities that may result from the large fields applied in such measurements and from the possible presence of mixed (electronic–ionic) conductivity. A recent study by Duijnstee *et al.* has pointed out that single-sweep SCLC transport characterization of halide perovskites may lead to a rather inaccurate assessment of their charge transport properties.[95] Additionally, the validation of SCLC data against the expected thickness dependence (e.g., with the inverse cube of the thickness, as per the Mott–Gurney law)—a tenet of robust SCLC transport analysis—is usually lacking. To ensure the accurate determination of charge transport data, it is therefore recommended that future SCLC investigations on lead-free perovskite absorbers should adopt (a) a double-sweep routine (i.e., comprising both forward and reverse scans), including pulsed biasing if hysteretic effects are pronounced,[95] and (b) the validation of the measured SCLC data against the expected model dependence on the semiconductor layer thickness.

Hall effect characterization is another approach that has also been widely adopted to experimentally determine the mobility of lead-free perovskite absorbers.[11,21,32,37,38,63,77,96–102] While its use with comparatively high-mobility and low-resistivity semiconductors is well-established, Hall effect characterization with a direct-current (DC, i.e., constant) magnetic field presents inherent challenges—and could be heavily impacted by measurement artifacts—when applied to high-resistivity, low-mobility ($<1\ cm^2\ V^{-1}\ s^{-1}$) semiconductors.[103,104] Taken aside the case of moderate/high-conductivity tin–germanium-based and tin-based perovskites,[32,77] DC-magnetic-field Hall effect characterization has nonetheless been pursued also with moderate/high-resistivity bismuth-based and antimony-based perovskite derivatives.[63,105] Considering that high-resistivity materials may lead to considerable experimental errors in the Hall effect parameter extraction,[104] it is advisable that future studies based on DC-magnetic-field Hall effect experiments should validate their data by critically assessing whether the expected trends are verified (e.g., in regard to the dependence of the carrier density and the Hall mobility on the magnetic field). On the other hand, Hall effect characterization relying on a modulated (AC) magnetic field has been demonstrated to offer a viable route to the characterization of low-mobility materials, down to a mobility range of $0.001\ cm^2\ V^{-1}\ s^{-1}$.[103] Such an AC characterization has been successfully reported in a few

instances in the recent literature on lead-free perovskites[37,38,101,102] and has the potential to become an attractive and widespread route to the charge transport characterization of lead-free perovskite absorbers.

E. Electronic dimensionality

In the search for high-performance lead-free perovskite absorbers, electronic dimensionality has been recognized as a key determinant of photovoltaic potential.[52] Indeed, higher electronic dimensionality has been related to superior charge transport properties, a higher defect tolerance, and reduced excitonic effects. Electronic dimensionality is determined by the connectivity of the orbitals contributing to the conduction and valence band edges. In many cases, electronic dimensionality overlaps with structural dimensionality (i.e., the structural connectivity of the perovskite network), e.g., as in 3D $ASnX_3$ and 0D Cs_2SnX_6. Along the same lines, bismuth-based and antimony-based $A_2B_3X_9$ systems are electronically 0.5D or 2.5D, depending on whether they are in their dimer or layered phase, respectively. Finally, in contrast to their structurally 3D character, cation-ordered double perovskites such as Cs_2AgBiX_6 are electronically 0D.

All things considered, apart from the electronically 3D $ASnX_3$ system (and taken aside the $AGeX_3$ system due to its inherent stability limitations), bismuth-based and antimony-based layered $A_2B_3X_9$ absorbers have the highest electronic dimensionality (2.5D) of all lead-free perovskites developed to date. This first highlights that the potential of antimony-based and bismuth-based $A_3Sb_2X_9$ absorbers should not be dismissed by narrowly referring only to their dimer-phase embodiments. It is of course puzzling that the PCE values of 2.5D $A_3Sb_2X_9$ and $A_3Bi_2X_9$ absorbers reported to date are, in fact, on par with or slightly lower than those of the 0.5D (dimer-phase) counterparts, as well as of the electronically 0D cation-ordered and vacancy-ordered double perovskites [Fig. 2(e)]. However, the literature on layered $A_3Sb_2X_9$ and $A_3Bi_2X_9$ reveals that their higher dimensionality compared to other classes of lead-free perovskites has not been truly exploited to date. Indeed, the photovoltaic implementations of layered $A_3B_2X_9$ demonstrated up to now have been realized with the planes of octahedra either predominantly parallel to the substrate or randomly oriented. Therefore, an outstanding question that needs to be addressed in order to exploit the 2.5D dimensionality of layered antimony-based and bismuth-based $A_2B_3X_9$ absorbers pertains to the development of deposition strategies for the favorable orientation of their planes of octahedra.

An additional dimensionality-related question that still needs to be addressed concerns the development of halide double perovskites that are electronically 3D (cf. electronically 0D character of Cs_2AgBiX_6). While some compositions with a low-toxicity profile that are expected to be electronically 3D have been proposed (e.g., indium–bismuth double perovskites),[106,107] to the best of our knowledge, no photovoltaic implementations based on such absorbers have been reported to date. Therefore, an important priority in halide double perovskite research pertains to the exploration of the photovoltaic properties of double perovskite embodiments that are electronically 3D, which are anticipated to enable a considerable increase in photovoltaic efficiency.

IV. OPPORTUNITIES

Lead-free halide perovskites are meant to address the toxicity concerns associated with their lead-based counterparts and concurrently provide opportunities for green photovoltaics. While lead-free perovskite research has thus far focused narrowly on investigating their capability for single-junction outdoor solar harvesting,[108] in fact, lead-free perovskites are potentially suitable for other applications in both indoor and outdoor photovoltaics (Fig. 4). Importantly, this potential is still largely unexplored. In this section, we present these photovoltaic opportunities, highlighting promising areas for future investigations that could enable lead-free perovskites to deliver their full photovoltaic potential.

A. Tandem photovoltaics

Lead-free perovskites are highly promising for silicon–perovskite tandem cell configurations. In consideration of their bandgap of ≈2 eV, lead-free absorbers with significant potential for perovskite–silicon tandem cells are antimony-based and bismuth-based $A_3B_2X_9$ perovskite derivatives, as well as cation-ordered double perovskites Cs_2AgBiX_6. The latter are particularly attractive also because of their comparatively large V_{oc} of ≈1 V under solar illumination. In regard to germanium-based perovskites, a potential route to tandem perovskite–silicon photovoltaics could be explored by pursuing wide-gap compositions through lighter halogens and/or alternative A-site cations.[28,29] In all of these cases, single or few layer graphene and 2D material electrodes may represent valid alternatives to the ITO top electrode and interconnection layer between the top perovskite and the bottom silicon cell, given the low transparency of ITO to near-infrared photons.

B. Indoor photovoltaics

The emergence of the Internet of Things (IoT)—with the rise of compact and energy-autonomous electronic devices such as wireless sensors and radio-frequency identification (RFID) tags—is expected to benefit from the availability of energy harvesters either in combination with or as an alternative to small energy storage devices (batteries, supercapacitors) in order to power the sensors and communicate via standard wireless radio modules and active RFIDs. Small (few cm^2) photovoltaic devices are expected to be commercialized for integration in IoT applications and represent a growing market opportunity for new technologies offering thin and flexible form factors. Photovoltaic cells located indoors with no access to solar illumination operate by harvesting the energy emitted by artificial light sources, with an illumination intensity 3 orders of magnitude lower than solar illumination, and different radiation spectra in the visible range depending on the light source. The optimum bandgap of photovoltaic absorbers required to match the emission spectra of both compact fluorescence lamps and white LED lamps is around 2.0 eV.[109] Importantly, this requirement matches the bandgap of many lead-free perovskites and derivatives (e.g., Cs_2AgBiX_6, antimony-based and bismuth-based $A_3B_2X_9$). Moreover, considering the comparatively low illumination levels relevant to indoor photovoltaics, the most promising absorbers are those that can deliver an ideality factor n close to unity, which requires the minimization of the bulk and interfacial defect state concentrations.[2,110] All things considered, the wide-bandgap nature of many

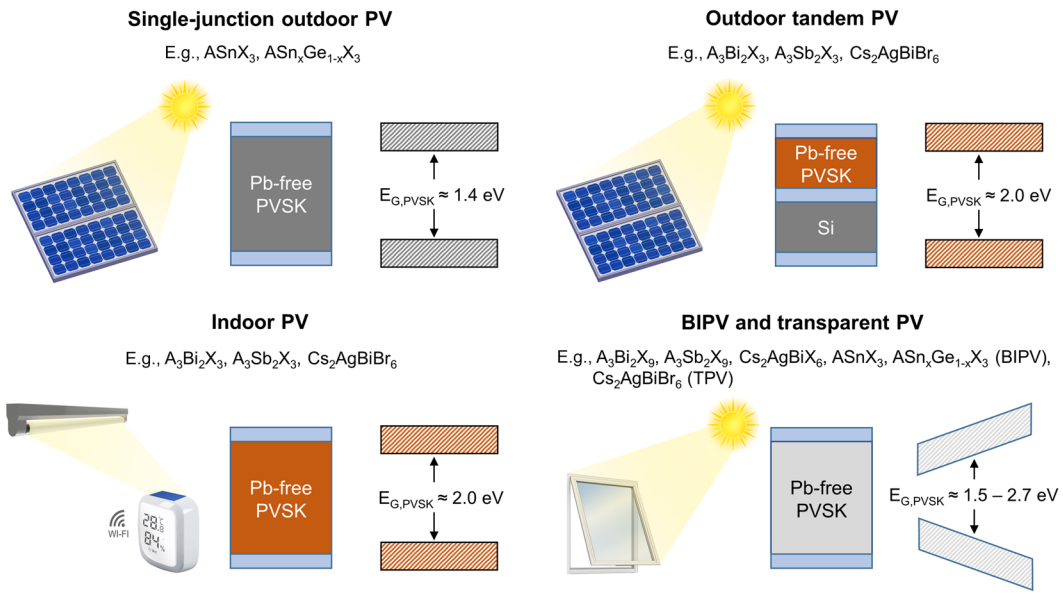

FIG. 4. Photovoltaic opportunities for lead-free perovskites.

lead-free perovskites points to their considerable potential as a green route to indoor photovoltaics and concurrently motivates future efforts toward deposition protocols enabling photoactive layers with a minimal concentration of recombination centers.

C. Building-integrated photovoltaics and transparent photovoltaics

The incorporation of transparent or semitransparent photovoltaic devices in different parts of buildings (e.g., facades, roofs, windows) opens up the prospect of harvesting solar energy while serving the esthetic and functional needs of the end-users. Lead-free perovskites come with colors covering different regions of the visible range, thereby providing attractive opportunities for color-tunable building-integrated photovoltaics (BIPV) applications in architectural design. In regard to transparent photovoltaics (TPV) for window applications, lead-free perovskites with a direct gap of around 2.7 eV would be particularly attractive in order to ensure high average visible transparency (AVT). Additionally, the adoption of indirect-gap double perovskite absorbers (e.g., Cs_2AgBiX_6) provides the opportunity to achieve high AVT with an optical gap of 2.0 eV, thereby concurrently allowing for the harvesting of visible light photons.[111] Finally, the full potential of lead-free perovskites for transparent photovoltaics could be realized by pursuing tandem configurations in combination with cells (e.g., organic) that absorb near-infrared photons.

V. CONCLUSIONS

Lead-free perovskites provide an attractive combination of perovskite-related optoelectronic properties with a generally low-toxicity profile. In recent years, considerable progress has been achieved in lead-free perovskite photovoltaics, notwithstanding a research effort of an incomparably smaller scale than that driving lead-based perovskite photovoltaics. Tin-based perovskites have delivered by far the highest single-junction PCE (≅13%) of all lead-free perovskites to date, and it can be envisaged that they may become an attractive technology provided that their stability is further improved and their toxicity profile is fully assessed. Another promising single-junction photovoltaics technology is represented by tin–germanium perovskites. Antimony/bismuth-based perovskite derivatives and double perovskites offer highly promising stability indications, but they require further development at the materials, processing, and device levels to further boost their performance.

In addition to general strategies that may lead to higher photovoltaic performance, in this Perspective, we have discussed a number of key open questions that pertain to the incomplete experimental assessment of the optoelectronic properties of lead-free perovskite absorbers. This involves first the widespread lack of Urbach energy data, which prevents detailed photovoltaic modeling and analysis of the dominant V_{oc} loss mechanism. Additionally, charge transport data are widely lacking, and the reliability of the charge transport data reported to date may require a critical re-assessment. A detailed experimental defect characterization of lead-free perovskites—aiming at the quantitative evaluation of defect densities, energies, and capture cross sections—has not been pursued to date, limiting the assessment of their defect tolerance, a property that closely relates to their photovoltaic potential. The impact of dimensionality and crystallographic orientation has not been fully assessed and exploited. Furthermore, standardized device stability data from lead-free perovskite solar cells are generally lacking, preventing the rational identification of the absorbers that are most promising from a stability point of view. All of these elements point to the need for a concerted effort toward a more in-depth experimental assessment of the optoelectronic properties and

stability of lead-free perovskite absorbers. By enabling detailed insight, such an effort would allow the identification of promising structures, compositions, and deposition protocols, ultimately catalyzing further progress in photovoltaic performance and stability.

While the bulk of the research on lead-free perovskites has narrowly focused on compositions and structures suitable for single-junction outdoor photovoltaics, this Perspective brings to the fore the manifold photovoltaic applications to which lead-free perovskites are also relevant. These involve tandem photovoltaics, indoor photovoltaics, and building-integrated and transparent photovoltaics. Importantly, these areas feature spectral requirements different from those of single-junction outdoor photovoltaics and may potentially offer a better match with the properties of many classes of lead-free perovskites. Therefore, we believe that for the full photovoltaic potential of lead-free perovskites to be realized, efforts should be directed at photovoltaic applications for which these absorbers truly represent an opportunity.

ACKNOWLEDGMENTS

This work was supported by the National Natural Science Foundation of China (Grant Nos. 61950410759 and 61805166), the Jiangsu Province Natural Science Foundation (Grant No. BK20170345), the Collaborative Innovation Center of Suzhou Nano Science & Technology, the Priority Academic Program Development of Jiangsu Higher Education Institutions (PAPD), the 111 Project, and the Joint International Research Laboratory of Carbon-Based Functional Materials and Devices.

DATA AVAILABILITY

The data that support the findings of this study are available from the corresponding author upon reasonable request.

REFERENCES

[1] A. K. Jena, A. Kulkarni, and T. Miyasaka, Chem. Rev. **119**, 3036 (2019).
[2] P. K. Nayak, S. Mahesh, H. J. Snaith, and D. Cahen, Nat. Rev. Mater. **4**, 269 (2019).
[3] Y. H. Kim, J. S. Kim, and T. W. Lee, Adv. Mater. **31**, 1970335 (2019).
[4] S. P. Senanayak, M. Abdi-Jalebi, V. S. Kamboj, R. Carey, R. Shivanna, T. Tian, G. Schweicher, J. Wang, N. Giesbrecht, D. Di Nuzzo, H. E. Beere, P. Docampo, D. A. Ritchie, D. Fairen-Jimenez, R. H. Friend, and H. Sirringhaus, Sci. Adv. **6**, eaaz4948 (2020).
[5] V. Pecunia, J. Phys. Mater. **2**, 042001 (2019).
[6] S. V. N. Pammi, R. Maddaka, V.-D. Tran, J.-H. Eom, V. Pecunia, S. Majumder, M.-D. Kim, and S. G. Yoon, Nano Energy **74**, 104872 (2020).
[7] See https://www.nrel.gov/pv/cell for National Renewable Energy Laboratory, 2020.
[8] R. Wang, M. Mujahid, Y. Duan, Z. K. Wang, J. Xue, and Y. Yang, Adv. Funct. Mater. **29**, 1808843 (2019).
[9] A. Abate, Joule **1**, 659 (2017).
[10] W. F. Yang, F. Igbari, Y. H. Lou, Z. K. Wang, and L. S. Liao, Adv. Energy Mater. **10**, 1902584 (2020).
[11] K. Nishimura, M. A. Kamarudin, D. Hirotani, K. Hamada, Q. Shen, S. Iikubo, T. Minemoto, K. Yoshino, and S. Hayase, Nano Energy **74**, 104858 (2020).
[12] W. Ke, C. C. Stoumpos, and M. G. Kanatzidis, Adv. Mater. **31**, 1803230 (2019).
[13] P. Xu, S. Chen, H.-J. Xiang, X.-G. Gong, and S.-H. Wei, Chem. Mater. **26**, 6068 (2014).
[14] N. K. Noel, S. D. Stranks, A. Abate, C. Wehrenfennig, S. Guarnera, A.-A. Haghighirad, A. Sadhanala, G. E. Eperon, S. K. Pathak, M. B. Johnston, A. Petrozza, L. M. Herz, and H. J. Snaith, Energy Environ. Sci. **7**, 3061 (2014).
[15] W. Ke and M. G. Kanatzidis, Nat. Commun. **10**, 965 (2019).
[16] M. E. Kayesh, T. H. Chowdhury, K. Matsuishi, R. Kaneko, S. Kazaoui, J.-J. Lee, T. Noda, and A. Islam, ACS Energy Lett. **3**, 1584 (2018).
[17] Q. Tai, X. Guo, G. Tang, P. You, T.-W. Ng, D. Shen, J. Cao, C.-K. Liu, N. Wang, Y. Zhu, C.-S. Lee, and F. Yan, Angew. Chem., Int. Ed. **58**, 806 (2019).
[18] X. Meng, T. Wu, X. Liu, X. He, T. Noda, Y. Wang, H. Segawa, and L. Han, J. Phys. Chem. Lett. **11**, 2965 (2020).
[19] T. Wang, Q. Tai, X. Guo, J. Cao, C.-K. Liu, N. Wang, D. Shen, Y. Zhu, C.-S. Lee, and F. Yan, ACS Energy Lett. **5**, 1741 (2020).
[20] E. Jokar, C.-H. Chien, C.-M. Tsai, A. Fathi, and E. W.-G. Diau, Adv. Mater. **31**, 1804835 (2019).
[21] M. A. Kamarudin, D. Hirotani, Z. Wang, K. Hamada, K. Nishimura, Q. Shen, T. Toyoda, S. Iikubo, T. Minemoto, K. Yoshino, and S. Hayase, J. Phys. Chem. Lett. **10**, 5277 (2019).
[22] W. Ke, C. C. Stoumpos, I. Spanopoulos, L. Mao, M. Chen, M. R. Wasielewski, and M. G. Kanatzidis, J. Am. Chem. Soc. **139**, 14800 (2017).
[23] W. Ke, C. C. Stoumpos, M. Zhu, L. Mao, I. Spanopoulos, J. Liu, O. Y. Kontsevoi, M. Chen, D. Sarma, Y. Zhang, M. R. Wasielewski, and M. G. Kanatzidis, Sci. Adv. **3**, e1701293 (2017).
[24] S. Shao, J. Liu, G. Portale, H.-H. Fang, G. R. Blake, G. H. ten Brink, L. J. A. Koster, and M. A. Loi, Adv. Energy Mater. **8**, 1702019 (2018).
[25] X. Jiang, F. Wang, Q. Wei, H. Li, Y. Shang, W. Zhou, C. Wang, P. Cheng, Q. Chen, L. Chen, and Z. Ning, Nat. Commun. **11**, 1245 (2020).
[26] F. Wang, X. Jiang, H. Chen, Y. Shang, H. Liu, J. Wei, W. Zhou, H. He, W. Liu, and Z. Ning, Joule **2**, 2732 (2018).
[27] H. Yao, F. Zhou, Z. Li, Z. Ci, L. Ding, and Z. Jin, Adv. Sci. **7**, 1903540 (2020).
[28] T. Krishnamoorthy, H. Ding, C. Yan, W. L. Leong, T. Baikie, Z. Zhang, M. Sherburne, S. Li, M. Asta, N. Mathews, and S. G. Mhaisalkar, J. Mater. Chem. A **3**, 23829 (2015).
[29] I. Kopacic, B. Friesenbichler, S. F. Hoefler, B. Kunert, H. Plank, T. Rath, and G. Trimmel, ACS Appl. Energy Mater. **1**, 343 (2018).
[30] K. A. Montiel, C. Yang, C. H. Andreasen, M. S. Gottlieb, M. R. Pfefferkorn, L. G. Wilson, J. L. W. Carter, and I. T. Martin, in *IEEE Photovoltaic Specialists Conference* (IEEE, 2019), p. 1183.
[31] M. Chen, M. G. Ju, H. F. Garces, A. D. Carl, L. K. Ono, Z. Hawash, Y. Zhang, T. Shen, Y. Qi, R. L. Grimm, D. Pacifici, X. C. Zeng, Y. Zhou, and N. P. Padture, Nat. Commun. **10**, 16 (2019).
[32] C. H. Ng, K. Nishimura, N. Ito, K. Hamada, D. Hirotani, Z. Wang, F. Yang, S. Likubo, Q. Shen, K. Yoshino, T. Minemoto, and S. Hayase, Nano Energy **58**, 130 (2019).
[33] T. Zhang, H. Li, H. Ban, Q. Sun, Y. Shen, and M. Wang, J. Mater. Chem. A **8**, 4118 (2020).
[34] Y. Yu, D. Zhao, C. R. Grice, W. Meng, C. Wang, W. Liao, A. J. Cimaroli, H. Zhang, K. Zhu, and Y. Yan, RSC Adv. **6**, 90248 (2016).
[35] P. Karuppuswamy, K. M. Boopathi, A. Mohapatra, H.-C. Chen, K.-T. Wong, P.-C. Wang, and C.-W. Chu, Nano Energy **45**, 330 (2018).
[36] M. Pazoki, M. B. Johansson, H. Zhu, P. Broqvist, T. Edvinsson, G. Boschloo, and E. M. J. Johansson, J. Phys. Chem. C **120**, 29039 (2016).
[37] Y. Peng, F. Li, Y. Wang, Y. Li, R. L. Z. Hoye, L. Feng, K. Xia, and V. Pecunia, Appl. Mater. Today **19**, 100637 (2020).
[38] F. Li, Y. Wang, K. Xia, R. L. Z. Hoye, and V. Pecunia, J. Mater. Chem. A **8**, 4396 (2020).
[39] B. Lee, A. Krenselewski, S. I. Baik, D. N. Seidman, and R. P. H. Chang, Sustainable Energy Fuels **1**, 710 (2017).
[40] W. Gao, C. Ran, J. Xi, B. Jiao, W. Zhang, M. Wu, X. Hou, and Z. Wu, ChemPhysChem **19**, 1696 (2018).
[41] M. Chen, M.-G. Ju, A. D. Carl, Y. Zong, R. L. Grimm, J. Gu, X. C. Zeng, Y. Zhou, and N. P. Padture, Joule **2**, 558 (2018).
[42] Y. Yang, C. Liu, M. Cai, Y. Liao, Y. Ding, S. Ma, X. Liu, M. Guli, S. Dai, and M. K. Nazeeruddin, ACS Appl. Mater. Interfaces **12**, 17062 (2020).

[43]B.-B. Yu, M. Liao, J. Yang, W. Chen, Y. Zhu, X. Zhang, T. Duan, W. Yao, S.-H. Wei, and Z. He, J. Mater. Chem. A **7**, 8818 (2019).
[44]X. He, T. Wu, X. Liu, Y. Wang, X. Meng, J. Wu, T. Noda, X. Yang, Y. Moritomo, H. Segawa, and L. Han, J. Mater. Chem. A **8**, 2760 (2020).
[45]S. M. Jain, D. Phuyal, M. L. Davies, M. Li, B. Philippe, C. De Castro, Z. Qiu, J. Kim, T. Watson, W. C. Tsoi, O. Karis, H. Rensmo, G. Boschloo, T. Edvinsson, and J. R. Durrant, Nano Energy **49**, 614 (2018).
[46]F. Bai, Y. Hu, Y. Hu, T. Qiu, X. Miao, and S. Zhang, Sol. Energy Mater. Sol. Cells **184**, 15 (2018).
[47]S. Weber, T. Rath, K. Fellner, R. Fischer, R. Resel, B. Kunert, T. Dimopoulos, A. Steinegger, and G. Trimmel, ACS Appl. Energy Mater. **2**, 539 (2019).
[48]E. Greul, M. L. Petrus, A. Binek, P. Docampo, and T. Bein, J. Mater. Chem. A **5**, 19972 (2017).
[49]X. Yang, Y. Chen, P. Liu, H. Xiang, W. Wang, R. Ran, W. Zhou, and Z. Shao, Adv. Funct. Mater. **30**, 2001557 (2020).
[50]F. Igbari, R. Wang, Z.-K. Wang, X.-J. Ma, Q. Wang, K.-L. Wang, Y. Zhang, L.-S. Liao, and Y. Yang, Nano Lett. **19**, 2066 (2019).
[51]R. Wang, J. Wang, S. Tan, Y. Duan, Z.-K. Wang, and Y. Yang, Trends Chem. **1**, 368 (2019).
[52]Z. Xiao, W. Meng, J. Wang, D. B. Mitzi, and Y. Yan, Mater. Horiz. **4**, 206 (2017).
[53]H. Hu, B. Dong, and W. Zhang, J. Mater. Chem. A **5**, 11436 (2017).
[54]B.-W. Park, B. Philippe, X. Zhang, H. Rensmo, G. Boschloo, and E. M. J. Johansson, Adv. Mater. **27**, 6806 (2015).
[55]J.-P. Correa-Baena, L. Nienhaus, R. C. Kurchin, S. S. Shin, S. Wieghold, N. T. Putri Hartono, M. Layurova, N. D. Klein, J. R. Poindexter, A. Polizzotti, S. Sun, M. G. Bawendi, and T. Buonassisi, Chem. Mater. **30**, 3734 (2018).
[56]J.-C. Hebig, I. Kühn, J. Flohre, and T. Kirchartz, ACS Energy Lett. **1**, 309 (2016).
[57]M. Abulikemu, S. Ould-Chikh, X. Miao, E. Alarousu, B. Murali, G. O. Ngongang Ndjawa, J. Barbé, A. El Labban, A. Amassian, and S. Del Gobbo, J. Mater. Chem. A **4**, 12504 (2016).
[58]K. M. Boopathi, P. Karuppuswamy, A. Singh, C. Hanmandlu, L. Lin, S. A. Abbas, C. C. Chang, P. C. Wang, G. Li, and C. W. Chu, J. Mater. Chem. A **5**, 20843 (2017).
[59]B. Saparov, F. Hong, J.-P. Sun, H.-S. Duan, W. Meng, S. Cameron, I. G. Hill, Y. Yan, and D. B. Mitzi, Chem. Mater. **27**, 5622 (2015).
[60]F. Umar, J. Zhang, Z. Jin, I. Muhammad, X. Yang, H. Deng, K. Jahangeer, Q. Hu, H. Song, and J. Tang, Adv. Opt. Mater. **7**, 1801368 (2019).
[61]A. Singh, K. M. Boopathi, A. Mohapatra, Y. F. Chen, G. Li, and C. W. Chu, ACS Appl. Mater. Interfaces **10**, 2566 (2018).
[62]F. Jiang, D. Yang, Y. Jiang, T. Liu, X. Zhao, Y. Ming, B. Luo, F. Qin, J. Fan, H. Han, L. Zhang, and Y. Zhou, J. Am. Chem. Soc. **140**, 1019 (2018).
[63]P. C. Harikesh, H. K. Mulmudi, B. Ghosh, T. W. Goh, Y. T. Teng, K. Thirumal, M. Lockrey, K. Weber, T. M. Koh, S. Li, S. Mhaisalkar, and N. Mathews, Chem. Mater. **28**, 7496 (2016).
[64]F. Igbari, Z. K. Wang, and L. S. Liao, Adv. Energy Mater. **9**, 1803150 (2019).
[65]P.-K. Kung, M.-H. Li, P.-Y. Lin, J.-Y. Jhang, M. Pantaler, D. C. Lupascu, G. Grancini, and P. Chen, Sol. RRL **4**, 1900306 (2020).
[66]X.-G. Zhao, D. Yang, J.-C. Ren, Y. Sun, Z. Xiao, and L. Zhang, Joule **2**, 1662 (2018).
[67]I. N. Flerov, M. V. Gorev, K. S. Aleksandrov, A. Tressaud, J. Grannec, and M. Couzi, Mater. Sci. Eng., R **24**, 81 (1998).
[68]R. Kentsch, M. Scholz, J. Horn, D. Schlettwein, K. Oum, and T. Lenzer, J. Phys. Chem. C **122**, 25940 (2018).
[69]L. Yu and A. Zunger, Phys. Rev. Lett. **108**, 068701 (2012).
[70]C. N. Savory, A. Walsh, and D. O. Scanlon, ACS Energy Lett. **1**, 949 (2016).
[71]A. H. Slavney, T. Hu, A. M. Lindenberg, and H. I. Karunadasa, J. Am. Chem. Soc. **138**, 2138 (2016).
[72]C. Wu, Q. Zhang, Y. Liu, W. Luo, X. Guo, Z. Huang, H. Ting, W. Sun, X. Zhong, S. Wei, S. Wang, Z. Chen, and L. Xiao, Adv. Sci. **5**, 1700759 (2018).
[73]M. R. Filip, X. Liu, A. Miglio, G. Hautier, and F. Giustino, J. Phys. Chem. C **122**, 158 (2018).
[74]S. E. Creutz, E. N. Crites, M. C. De Siena, and D. R. Gamelin, Nano Lett. **18**, 1118 (2018).
[75]F. Wei, Z. Deng, S. Sun, N. T. P. Hartono, H. L. Seng, T. Buonassisi, P. D. Bristowe, and A. K. Cheetham, Chem. Commun. **55**, 3721 (2019).
[76]W. Meng, X. Wang, Z. Xiao, J. Wang, D. B. Mitzi, and Y. Yan, J. Phys. Chem. Lett. **8**, 2999 (2017).
[77]X. Qiu, B. Cao, S. Yuan, X. Chen, Z. Qiu, Y. Jiang, Q. Ye, H. Wang, H. Zeng, J. Liu, and M. G. Kanatzidis, Sol. Energy Mater. Sol. Cells **159**, 227 (2017).
[78]T. Kirchartz and U. Rau, Adv. Energy Mater. **8**, 1703385 (2018).
[79]J. Euvrard, X. Wang, T. Li, Y. Yan, and D. B. Mitzi, J. Mater. Chem. A **8**, 4049 (2020).
[80]D. Sabba, H. K. Mulmudi, R. R. Prabhakar, T. Krishnamoorthy, T. Baikie, P. P. Boix, S. Mhaisalkar, and N. Mathews, J. Phys. Chem. C **119**, 1763 (2015).
[81]W. Ming, H. Shi, and M.-H. Du, J. Mater. Chem. A **4**, 13852 (2016).
[82]S. Nagane, D. Ghosh, R. L. Z. Hoye, B. Zhao, S. Ahmad, A. B. Walker, M. S. Islam, S. Ogale, and A. Sadhanala, J. Phys. Chem. C **122**, 5940 (2018).
[83]A. J. Lehner, D. H. Fabini, H. A. Evans, C.-A. Hébert, S. R. Smock, J. Hu, H. Wang, J. W. Zwanziger, M. L. Chabinyc, and R. Seshadri, Chem. Mater. **27**, 7137 (2015).
[84]T. Miyasaka, A. Kulkarni, G. M. Kim, S. Öz, and A. K. Jena, Adv. Energy Mater. **10**, 1902500 (2020).
[85]Q. Jiang, Y. Zhao, X. Zhang, X. Yang, Y. Chen, Z. Chu, Q. Ye, X. Li, Z. Yin, and J. You, Nat. Photonics **13**, 460 (2019).
[86]M. Kim, G.-H. Kim, T. K. Lee, I. W. Choi, H. W. Choi, Y. Jo, Y. J. Yoon, J. W. Kim, J. Lee, D. Huh, H. Lee, S. K. Kwak, J. Y. Kim, and D. S. Kim, Joule **3**, 2179 (2019).
[87]M. V. Khenkin, E. A. Katz, A. Abate, G. Bardizza, J. J. Berry, C. Brabec, F. Brunetti, V. Bulović, Q. Burlingame, A. Di Carlo, R. Cheacharoen, Y.-B. Cheng, A. Colsmann, S. Cros, K. Domanski, M. Dusza, C. J. Fell, S. R. Forrest, Y. Galagan, D. Di Girolamo, M. Grätzel, A. Hagfeldt, E. von Hauff, H. Hoppe, J. Kettle, H. Köbler, M. S. Leite, S. Liu, Y.-L. Loo, J. M. Luther, C.-Q. Ma, M. Madsen, M. Manceau, M. Matheron, M. McGehee, R. Meitzner, M. K. Nazeeruddin, A. F. Nogueira, Ç. Odabaşı, A. Osherov, N.-G. Park, M. O. Reese, F. De Rossi, M. Saliba, U. S. Schubert, H. J. Snaith, S. D. Stranks, W. Tress, P. A. Troshin, V. Turkovic, S. Veenstra, I. Visoly-Fisher, A. Walsh, T. Watson, H. Xie, R. Yıldırım, S. M. Zakeeruddin, K. Zhu, and M. Lira-Cantu, Nat. Energy **5**, 35 (2020).
[88]R. E. Brandt, J. R. Poindexter, P. Gorai, R. C. Kurchin, R. L. Z. Hoye, L. Nienhaus, M. W. B. Wilson, J. A. Polizzotti, R. Sereika, R. Žaltauskas, L. C. Lee, J. L. MacManus-Driscoll, M. Bawendi, V. Stevanović, and T. Buonassisi, Chem. Mater. **29**, 4667 (2017).
[89]A. M. Ganose, C. N. Savory, and D. O. Scanlon, Chem. Commun. **53**, 20 (2017).
[90]T. N. Huq, L. C. Lee, L. Eyre, W. Li, R. A. Jagt, C. Kim, S. Fearn, V. Pecunia, F. Deschler, J. L. MacManus-Driscoll, and R. L. Z. Hoye, Adv. Funct. Mater. **30**, 1909983 (2020).
[91]R. E. Brandt, V. Stevanović, D. S. Ginley, and T. Buonassisi, MRS Commun. **5**, 265 (2015).
[92]Y. Li, D. Maldonado-Lopez, V. Ríos Vargas, J. Zhang, and K. Yang, J. Chem. Phys. **152**, 084106 (2020).
[93]C. Ran, Z. Wu, J. Xi, F. Yuan, H. Dong, T. Lei, X. He, and X. Hou, J. Phys. Chem. Lett. **8**, 394 (2017).
[94]X.-L. Li, L.-L. Gao, B. Ding, Q.-Q. Chu, Z. Li, and G.-J. Yang, J. Mater. Chem. A **7**, 15722 (2019).
[95]E. A. Duijnstee, J. M. Ball, V. M. Le Corre, L. J. A. Koster, H. J. Snaith, and J. Lim, ACS Energy Lett. **5**, 376 (2020).
[96]C. K. Liu, Q. Tai, N. Wang, G. Tang, H. L. Loi, and F. Yan, Adv. Sci. **6**, 1900751 (2019).
[97]I. Chung, J. Song, J. Im, J. Androulakis, C. D. Malliakas, H. Li, A. J. Freeman, J. T. Kenney, and M. G. Kanatzidis, J. Am. Chem. Soc. **134**, 8579 (2012).
[98]M. H. Kumar, S. Dharani, W. L. Leong, P. P. Boix, R. R. Prabhakar, T. Baikie, C. Shi, H. Ding, R. Ramesh, M. Asta, M. Graetzel, S. G. Mhaisalkar, and N. Mathews, Adv. Mater. **26**, 7122 (2014).
[99]B. Saparov, J. P. Sun, W. Meng, Z. Xiao, H. S. Duan, O. Gunawan, D. Shin, I. G. Hill, Y. Yan, and D. B. Mitzi, Chem. Mater. **28**, 2315 (2016).

[100]K. Nishimura, D. Hirotani, M. A. Kamarudin, Q. Shen, T. Toyoda, S. Iikubo, T. Minemoto, K. Yoshino, and S. Hayase, ACS Appl. Mater. Interfaces **11**, 31105 (2019).
[101]P. C. Harikesh, B. Wu, B. Ghosh, R. A. John, S. Lie, K. Thirumal, L. H. Wong, T. C. Sum, S. Mhaisalkar, and N. Mathews, Adv. Mater. **30**, 1802080 (2018).
[102]V. Pecunia, Y. Yuan, J. Zhao, K. Xia, Y. Wang, S. Duhm, L. Portilla, and F. Li, Nano-Micro Lett. **12**, 27 (2020).
[103]J. Lindemuth and S.-I. Mizuta, Proc. SPIE **8110**, 81100I (2011).
[104]F. Werner, J. Appl. Phys. **122**, 135306 (2017).
[105]S.-Y. Kim, Y. Yun, S. Shin, J. H. Lee, Y.-W. Heo, and S. Lee, Scr. Mater. **166**, 107 (2019).
[106]Z. Xiao, Y. Yan, H. Hosono, and T. Kamiya, J. Phys. Chem. Lett. **9**, 258 (2018).
[107]G. Volonakis, A. A. Haghighirad, H. J. Snaith, and F. Giustino, J. Phys. Chem. Lett. **8**, 3917 (2017).
[108]H. Fu, Sol. Energy Mater. Sol. Cells **193**, 107 (2019).
[109]I. Mathews, S. N. Kantareddy, T. Buonassisi, and I. M. Peters, Joule **3**, 1415 (2019).
[110]W. Tress, M. Yavari, K. Domanski, P. Yadav, B. Niesen, J. P. Correa Baena, A. Hagfeldt, and M. Graetzel, Energy Environ. Sci. **11**, 151 (2018).
[111]G. Liu, C. Wu, Z. Zhang, Z. Chen, L. Xiao, and B. Qu, Sol. RRL **4**, 2000056 (2020).